pubs.acs.org/Biomac

Article

Synthesis of Poly(allyl glycidyl ether)-Derived Polyampholytes and Their Application to the Cryopreservation of Living Cells

Aaron A. Burkey, Neda Ghousifam, Alexander V. Hillsley, Zachary W. Brotherton, Mahboobeh Rezaeeyazdi, Taylor A. Hatridge, Dale T. Harris, William W. Sprague, Brittany E. Sandoval, Adrianne M. Rosales, Marissa Nichole Rylander, and Nathaniel A. Lynd*

Cite This: *Biomacromolecules* 2023, 24, 1475−1482

Read Online

ACCESS | Metrics & More | Article Recommendations | Supporting Information

ABSTRACT: Through the postpolymerization modification of poly(allyl glycidyl ether) (PAGE), a functionalizable polyether with a poly(ethylene oxide) backbone, we engineered a new class of highly tunable polyampholyte materials. These polyampholytes can be synthesized to have several useful properties, including low cytotoxicity and pH-responsive coacervate formation. In this study, we used PAGE-based polyampholytes (PAGE-PAs) for the cryopreservation of mammalian cell suspensions. Typically, dimethyl sulfoxide (DMSO) is the cryoprotectant used for preserving mammalian cells, but DMSO suffers from key drawbacks including toxicity and difficult post-thaw removal that motivates the development of new materials and methods. Toxicity and post-thaw survival were dependent on PAGE-PA composition with the highest immediate post-thaw survival for normal human dermal fibroblasts occurring for the least toxic PAGE-PA at a cation/anion ratio of 35:65. With low toxicity, the PAGE-PA concentration could be increased in order to increase immediate post-thaw survival of the immortalized mouse embryonic fibroblasts (NIH/3T3). While immediate post-thaw viability was achieved using only the PAGE-PAs, long-term cell survival was low, highlighting the challenges involved with the design of cryoprotective polyampholytes. An environment utilizing both PAGE-PAs and DMSO in a cryoprotective solution offered promising post-thaw viabilities exceeding 70%, with long-term metabolic activities comparable to unfrozen cells.

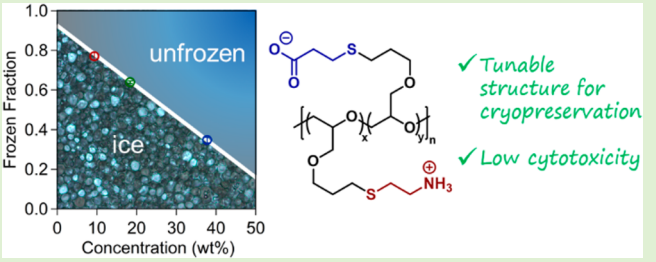

INTRODUCTION

Improved cryoprotectant materials are necessary to improve the long-term frozen storage of living cells and tissue.[1] Traditionally, organic solvents such as dimethyl sulfoxide (DMSO) or glycerol are used to promote post-thaw cell survival. As ice forms outside of a cell, solutes are excluded into the interstitial space between the growing ice crystals, exerting osmotic stress on cells. DMSO can cross the cell membrane to balance osmotic pressure, effectively replacing intracellular water and reducing the likelihood of lethal intracellular ice formation.[2,3] Membrane penetrating cryoprotectants like DMSO have two key drawbacks: They are cytotoxic, and post-thaw removal requires intracellular DMSO to cross the cell membrane a second time, exerting a new set of osmotic stresses.[3]

Polymeric cryoprotectants, on the other hand, do not readily cross the cell membrane owing to their large size. For this reason, the mechanism by which they promote post-thaw cell survival may be fundamentally different than that of DMSO. When using polymeric cryoprotectants, enough water must be osmotically drawn from a cell to inhibit intracellular ice formation, but not so much water that cells face damage from dehydration.[4] In this situation, polymeric materials have the advantage of filling volume that would otherwise be ice without exerting significant osmotic pressure across the cell membrane because of their high molecular weight. Some polymeric cryoprotectants, most notably poly(vinyl alcohol) (PVA), inhibit the Ostwald ripening of ice, which is believed to impart mechanical stresses on cells during thawing.[5−17] Other polymers with little to no effect on Ostwald ripening have also been employed as cryoprotectants.[18−25] For example, hydroxyethyl starch,[6,21] poly(glycerol monomethacrylate)-*b*-poly(2-hydroxypropyl methacrylate),[26] and polyvinylpyrrolidone[27] have been used at 5−20 wt % to preserve red blood cells. Additionally, poly(ethylene oxide) has been employed as a cryoprotectant for *E. coli*,[28] alginate hydrogels have been used to encapsulate stem cells for frozen storage,[29] and polymers with sulfoxide-appended backbones have been shown to

Received: December 16, 2022
Revised: January 28, 2023
Published: February 13, 2023

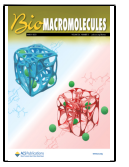

promote superior recovery and viability in A549,[30] 3T3, and NHDF cells.[17]

A handful of cryoprotective polyampholytes, polymers bearing both positive and negative charges, have been developed.[31−37] It is suggested that these polymers promote post-thaw cell survival by stabilizing the cell membrane and inhibiting ice grain coarsening during freezing and thawing.[38,39] Herein, we present a straightforward synthetic platform that can be applied to make a broad array of compositionally diverse polyampholyte materials. These new polyampholytes were nontoxic at a concentration of 10 wt %, and enabled immediate post-thaw recovery of mammalian cells on par with DMSO, but failed to achieve long-term post-thaw cell survival, except when used in combination with DMSO.

EXPERIMENTAL SECTION

Materials. Allyl glycidyl ether (TCI, >99%) was vacuum distilled over calcium hydride prior to use. Dimethylformamide (DMF; Fisher, Cert. ACS), ethyl acetate (Fisher, Cert. ACS), mercaptopropionic acid (Alfa Aesar), cysteamine hydrochloride (Acros, 98%), octanethiol (TCI, 98%), naphthalene (Aldrich, >99%), potassium (Aldrich, 98% in mineral oil), and azobis(isobutyronitrile) (AIBN; Aldrich, 98%) were used as received.

Equipment. Size exclusion chromatography (SEC) was carried out on an Agilent system with a 1260 Infinity isocratic pump, degasser, and thermostatted column chamber held at 30 °C containing Agilent 5 μm MIXED-C columns with a combined operating range of 200−2000000 g mol^{-1} relative to polystyrene standards. Chloroform with 50 ppm amylene was used as the mobile phase. The SEC system was equipped with an Agilent 1260 Infinity refractometer and dynamic and static light scattering. ^{1}H NMR spectroscopy was performed on a 400 MHz Agilent MR spectrometer at room temperature and referenced to the residual solvent signal of $CDCl_3$ or D_2O (7.26 and 4.79 ppm, respectively). Ice recrystallization kinetic assays were performed using a Zeiss Axio Scope.A1 with a 10× N-Achroplan objective and a Linkam LTS420 temperature-controlled stage. Differential scanning calorimetry was performed using a DSC250 (TA Instruments) with an RCS90 electric chiller.

Synthesis of Poly(allyl glycidyl ether). Poly(allyl glycidyl ether) (PAGE) was synthesized via anionic polymerization using an adapted version of a previously reported method.[40] A total of 230 μL of benzyl alcohol was added to a sealed reactor under an inert atmosphere. The benzyl alcohol was titrated with a 0.3 M solution of potassium naphthalenide in THF until a green color persisted. Allyl glycidyl ether (50 g) was added by buret, and the polymerization was allowed to continue for at least 3 days at 45 °C. The resulting PAGE was purified by precipitation in hexanes and dried under vacuum. M_n = 16.0 kg/mol, Đ = 1.2.

Polyampholyte Synthesis. In a representative procedure, 5 g of PAGE was dissolved in 50 mL of DMF. Cysteamine hydrochloride, mercaptopropionic acid, and octanethiol were each added to the mixture in 1.2× molar excess with respect to the number of allyl groups to be modified by each thiol. A 0.1 mol equiv of AIBN was added for every mole of alkene. The mixture was bubbled with N_2 for 10 min and stirred at 70 °C for 20−24 h. The resulting polyampholyte was precipitated in ethyl acetate, dialyzed in deionized water for at least 4 days, frozen in liquid nitrogen, and lyophilized. Polyampholyte solutions became turbid during dialysis, likely due to the formation of coacervate phases. Ratios of amine units to carboxylic acid units were verified using ^{1}H NMR spectroscopy. Polymer characterization by NMR and GPC is shown in Figures S1−S9. Ratios of carboxylic acid to amine groups (as measured by NMR) were within two percentage points of the target ratio (Figure S9).

Cell Culture. Primary normal human dermal fibroblasts (NHDF, Promocell) and immortalized mouse embryonic fibroblast (NIH/3T3, American Type Cultural Collection) cells were cultured in the designated supplemented culture medium (complete medium), incubated at standard conditions (37 °C and humidified atmosphere of 5% CO_2), and used at 90% confluence for sample preparations. For all experiments, cells were used between passages 5 and 15.

Cytotoxicity Assay. NHDF cells were seeded at 20000 cells/mL in solid 96-well plates (Corning Life Sciences), incubated under standard conditions, and used for experiments after cells achieved confluence, as confirmed by microscopic observation. PAGE-PAs with different amine to carboxylic acid ratios (50:50, 45:55, 40:60, and 35:65) were dissolved in complete medium to the final concentration of 10 wt %, followed by pH adjustment to 7.4 using 10 M NaOH. Solutions were added on the cell layer and incubated at standard conditions for 24 h. NHDF viability was measured at the end of the incubation time using CellTiter-Blue assay (Promega). Complete medium and 10 vol % DMSO (Fisher Scientific) were used as negative and positive controls, respectively.

Cryopreservation Protocol and Post-Thaw Viability Assay. PAGE-PAs with different amine to carboxylic acid ratios (50:50, 45:55, 40:60, and 35:65) were dissolved in phosphate-buffered saline (PBS, Sigma-Aldrich) with 1% penicillin/streptomycin (Hyclone) to the desired concentration. Solution pH was adjusted as previously described. Cells were suspended in PAGE-PA solutions to the final concentration of 0.5 × 10^6 cells/mL (Figure 2a) or 1 × 10^6 (Figures 2c and 3a), cooled to −80 °C at a rate of 1 °C/min (Mr. Frosty, Nalgene), and stored at −80 °C for a minimum of 4 h. Cryovials were then transferred to a liquid nitrogen container and stored for at least 24 h before thawing. As with cytotoxicity experiments, a complete medium and 10 vol % DMSO were used as negative and positive controls, respectively.

Vials were thawed by immersing into a water bath (37 °C) for 2 min. Then, cell suspensions were transferred to centrifuge tubes containing complete medium and centrifuged for 3 min at 220 × g to remove cryoprotectants. Fresh complete medium was added to the cells, and samples were incubated at 37 °C for 1.5 h to allow for recovery. For the polymer concentration sweep shown in Figure 2c, this incubation period was not included. At the end of the incubation time, the number of viable cells was counted using a trypan blue exclusion assay. Post-thaw cell survival yield values were reported as a ratio of viable cells counted after thawing to the initial cells in each cryovial. Raw data for post-thaw cell survival is included in Table S1.

For the post-thaw proliferation studies, 10000 live NHDF cells were isolated from each condition and plated in a 96-well plate (3 wells of 10000 cells per condition). Cells were then cultured for 4, 28, 52, or 76 h under standard conditions. At the desired time point, the media was removed and replaced with phenol-free Dulbecco's Modified Eagle Medium (DMEM; no FBS) with 1.2 mM MTT solution (Invitrogen). After a 4 h incubation, a solution of 10% (w/v) SDS and 0.01 M HCl was added to solubilize the formazan product. Absorbance was then measured at 570 nm using a plate reader (BioTek) as a measure of cell mitochondria activity. Nonfrozen cells were plated and used as a control in all proliferation studies.

For trials in which one cell culture was treated with both DMSO and PAGE-PA, human fibroblast cells were frozen in complete media containing 7% w/v PAGE-PA(35:65:0) + 3% w/v DMSO, held at −80 °C for 24 h, and then frozen in liquid nitrogen for 1 week before thawing. The cells were washed and plated in 96-well plates with an initial density of 5000/cm^2 and incubated at 37 °C for 72 h, over which the metabolic activity of the cells was monitored as described above.

Differential Scanning Calorimetry (DSC). Polyampholyte solutions were prepared at multiple concentrations in phosphate-buffered saline (PBS). A 10 M NaOH solution was used to adjust the pH to 7.4. For each solution, 5−10 mg of solution was loaded into hermetically sealed aluminum DSC pans. Samples were frozen by cooling at a rate of 5 °C/min to −90 °C, then reheated to 20 °C at 10 °C/min. Glass transition temperatures and peak integrals were determined using Trios software. A sigmoidal baseline was used when integrating melting peaks. All trials were performed in triplicate. Raw DSC traces are included in Figures S10−S12.

Ice Recrystallization Inhibition Measurement. A "splat" ice recrystallization assay was adapted from that of Knight et al.[41,42] A 20 μL droplet was expelled from a height of 1.5 m onto a microscope

https://doi.org/10.1021/acs.biomac.2c01488
Biomacromolecules 2023, 24, 1475−1482

slide chilled to −78 °C with dry ice, then quickly transferred to a microscope stage held at −6 °C. Images were collected after annealing for 30 min to allow ample time for ice recrystallization to occur. Ice samples were illuminated with cross-polarized light. The mean largest grain size (MLGS) represents the average longest linear dimension of the largest crystal within the field of view for each trial after annealing, measured manually using ImageJ. Three trials were performed for each material. Cryoprotectant concentrations were 10 wt %.

Statistical Analysis. All data are expressed as mean ± standard deviation. For the post-thaw survival assays, an independent experiment constitutes one freeze/thaw cycle of cells from the same passage on the same day. All experiments were conducted in at least duplicate (at least two technical repeats), and a minimum of three independent experiments were performed for statistical analysis. To compare data among three groups or more, a one-way analysis of variance (ANOVA) was used. To compare data among two groups, a two-tailed *t* test (assuming unequal variance) was used. A *p* value of <0.05 was considered statistically significant.

RESULTS AND DISCUSSION

Polyampholytes were derived from poly(allyl glycidyl ether) (PAGE) using thiol−ene chemistry, as shown in Scheme 1. A

Scheme 1. Synthesis of PAGE-PA Cryoprotectants is Achieved Through Thiol−ene Modification of PAGE

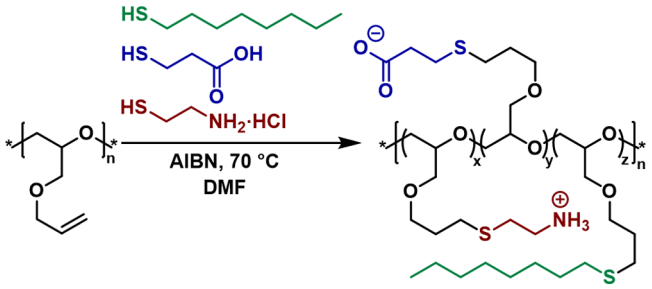

similar approach has been employed to make polyelectrolytes with LCST[43] or complex-forming properties[44−46] but, to the best of the authors' knowledge, has never been used to make polyampholyte materials. A key advantage of PAGE-derived polyampholytes, referred to throughout as PAGE-PAs, is that their composition is highly tunable: Virtually any thiol can be substituted for those shown in Scheme 1, and their ratios can be varied by simply changing the relative concentration of thiol reagents. A representative ^{1}H NMR spectrum for PAGE-PA with 35% amine-bearing repeat units and 65% carboxylic acid-bearing repeat units is shown in Figure 1. Interestingly, the PAGE-PAs were shown to have composition-dependent pH-responsive coacervate formation (Figure S13), but coacervate phases were only observed at pH values lower than those used for cryopreservation (pH = 7.4).

At 10 wt %, PAGE-PA had optimal cryoprotective capabilities when the amine to carboxylic acid ratio was 35:65, as shown in Figure 2a. Post-thaw cell survival was comparable with that achieved using DMSO, the most routinely used cryoprotectant for mammalian cells. For the PAGE-PAs, improved cell viability can be partly attributed to lower toxicity at higher carboxylic acid content. Cation-rich polymers are sometimes employed as antimicrobial agents,[47] so it is likely that excessively amine-rich polyampholytes are similarly toxic. Indeed, we observed that cation-rich polyampholytes were somewhat toxic to fibroblast cells, but anion-rich polyampholytes were almost entirely nontoxic (Figure 2b). Matsumura and co-workers similarly observed the best

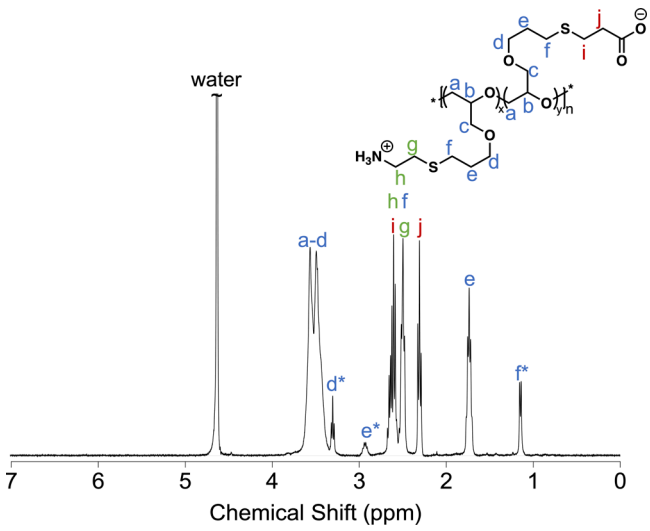

Figure 1. ^{1}H NMR spectrum of PAGE-PA; x = 0.35, y = 0.65. Solvent was D_2O with 0.1 M NaOH added to promote solubility. Labels with asterisks correspond to repeat units in which mercaptopropionic acid reacted with the nonterminal carbon of the PAGE pendant group.

post-thaw cell survival at a cation to anion ratio of 35:65 with poly(L-lysine)-derived polyampholytes. They attributed the higher post-thaw viability to better restriction of ice grain coarsening,[31] but unlike other polyampholyte materials,[31,48] the cation/anion ratio of the PAGE-PAs had little to no influence on ice grain size (Figure 5).

Different cell types varied in response when PAGE-PAs were used as cryoprotectants, possibly due to differences in polymer/membrane interactions, tolerance to high osmotic pressure, or rate of water transport across the cell membrane.[49] 3T3 cells showed poor post-thaw viability in the presence of 10 wt % PAGE-PA, but the low toxicity of the polymer solution made it feasible to increase the polymer concentration until appreciable cell recovery was achieved. Since a high polymer mass concentration corresponds to a relatively low molar concentration, osmotic effects from a highly concentrated cryoprotectant are minimal compared to small molecules such as DMSO or trehalose. There may be room for further improvement of post-thaw viability by optimizing the concentration of PAGE-PAs.

Some authors have reported higher post-thaw cell viabilities than those shown in Figure 2 when using polyampholytes as cryoprotectants.[31,32,34,38] These authors generally also reported higher post-thaw cell viabilities of 80−90% when using DMSO alone as a cryoprotectant. These differences could likely be attributed to differences in delay after thawing before measuring viability, robustness of different cell lines, and variation in normalization methods during cell counting.[50]

Incorporation of hydrophobic units into cryoprotective polyampholytes has also been shown to improve performance for methacrylate-based polyampholytes. We therefore used alkyl thiols to impart similar functionality to PAGE-PAs.[38] In contrast to previously reported cryoprotective polyampholytes, incorporation of octyl units reduced post-thaw cell viability (Figure 3a). Additionally, PAGE-PAs with octyl groups were seen to give almost no long-term post-thaw recovery (Figure 3b). PAGE-PA with no octyl groups gave some long-term post-thaw recovery, but DMSO performed better in the long term. Other authors have similarly observed that polyampholytes alone were unable to achieve long-term post-thaw cell survival,

https://doi.org/10.1021/acs.biomac.2c01488
Biomacromolecules 2023, 24, 1475−1482

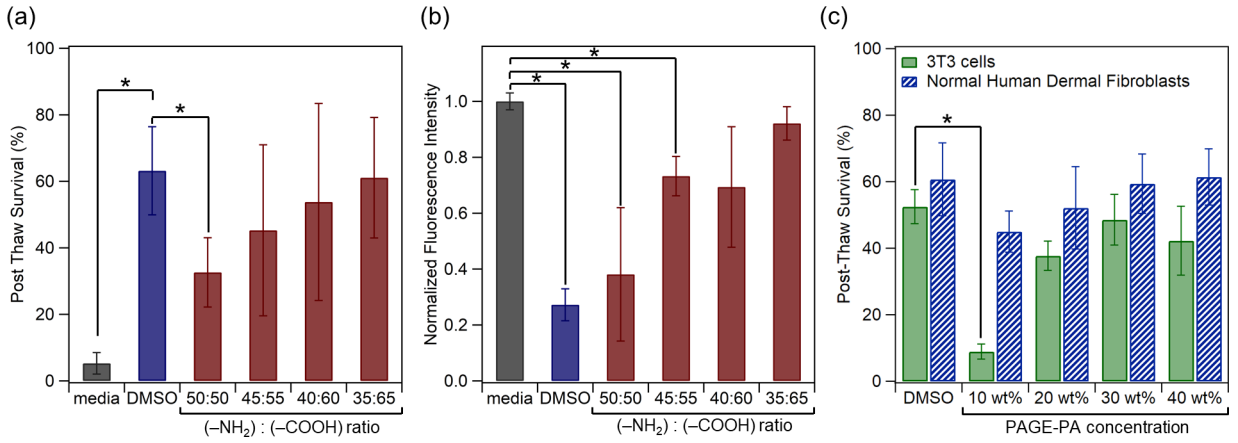

Figure 2. (a) Post-thaw NHDF cell survival yield shows that PAGE-PA with a 35:65 amine to carboxylic acid ratio had immediate post-thaw survival comparable to DMSO. Error bars represent standard deviation among three independent experiments (three samples per experiment). All polymer concentrations are 10 wt %. DMSO concentration is 10 vol %. (b) Carboxylic acid-rich PAGE-PAs exhibit low cytotoxicity. NHDF cell viability was measured by CellTiter-Blue assay after incubating samples at 37 °C for 24 h. Error bars represent the standard deviation of four independent experiments (three samples per experiment). All polymer concentrations are 10 wt %. DMSO concentration is 10 vol %. (c) For 3T3 cells, PAGE-PA (35:65) was a poor cryoprotectant at 10 wt %. However, the cytotoxicity of PAGE-PA was low enough that the concentration can be increased until appreciable cell viability was achieved. Increased PAGE-PA concentration led to modest improvement in cell viability for NHDF cells. Error bars represent the standard deviation among three independent experiments (two samples per trial). Asterisks denote post-thaw cell viabilities significantly different compared to that achieved with DMSO ($p < 0.05$).

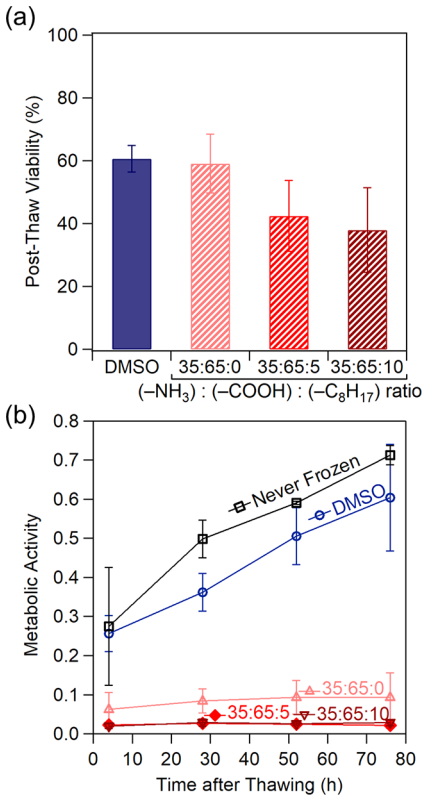

Figure 3. (a) Octyl-functional PAGE-PAs did not lead to improved post-thaw NHDF cell viability, as determined by a trypan blue exclusion assay immediately after thawing. (b) When equal numbers of live NHDF cells were plated after thawing to assess long-term viability, metabolic activity (measured by MTT absorbance assay) was lower for cells preserved with PAGE-PAs than those preserved with DMSO. Incorporation of hydrophobic functionality (ratio of $-NH_3$/$-COOH$/$-C_8H_{17}$ groups is indicated above curve) decreased long-term cell viability. In all trials, DMSO concentration was 10 vol % and PAGE-PA concentration was 10 wt %. At least four independent experiments were performed for each condition.

but they reported that including membrane-penetrating cryoprotectants in addition to cryoprotective polyampholytes led to improved recovery.[34,51,52]

Compared to the traditional cryoprotectant DMSO, PAGE-PAs offer the advantage of low cytotoxicity and equivalent post-thaw viability at the cost of long-term metabolic activity. In recognition of this trade-off and following literature motifs,[32,35,44,45,53] there is merit to combining PAGE-PA with a small amount of DMSO to assess any synergistic or noncooperative effects on cell recovery. A 7% w/v of the optimal PAGE-PA 35:65 ratio of amines to carboxylic acid was combined with 3% w/v DMSO for trials reported in Figure 4. The combination of PAGE-PA and DMSO allowed for increased post-thaw viability compared to DMSO or PAGE-PA alone and demonstrated a significant increase in long-term metabolic activity above that of the PAGE-PA and approaching that of never-frozen cells. This increase in post-thaw and long-term viability can be attributed to the reduction of cytotoxic DMSO in the media while maintaining an active concentration of cryoprotectant both intra- and extracellularly. These results are consistent with similar studies using different PA materials on stem cells performed by Murray et al.[53]

Ice recrystallization inhibition (IRI) is frequently investigated as a key feature of polymeric cryoprotectants. Ice recrystallization, a form of Ostwald ripening, is the process in which average crystal size increases to reduce surface energy. Using PVA, an excellent IRI agent, in combination with other cryoprotectants significantly increased post-thaw cell viability in several studies.[6,26,54,55] Ice crystal size in the presence of PAGE-PAs was smaller than in the absence of polymer, likely due to increased viscosity and decreased diffusivity of the space between the ice crystals. None of the PAGE-PAs displayed any IRI activity beyond that of poly(ethylene oxide) (PEO), a polymer with minimal IRI activity (Figure 5).

Unsurprisingly, increasing the mass fraction of 35:65 PAGE-PA decreased the total amount of ice that formed, as shown in Figure 6a,b. By reducing the volume of ice, the degree to which solutes can be concentrated in the space between ice crystals

https://doi.org/10.1021/acs.biomac.2c01488
Biomacromolecules 2023, 24, 1475−1482

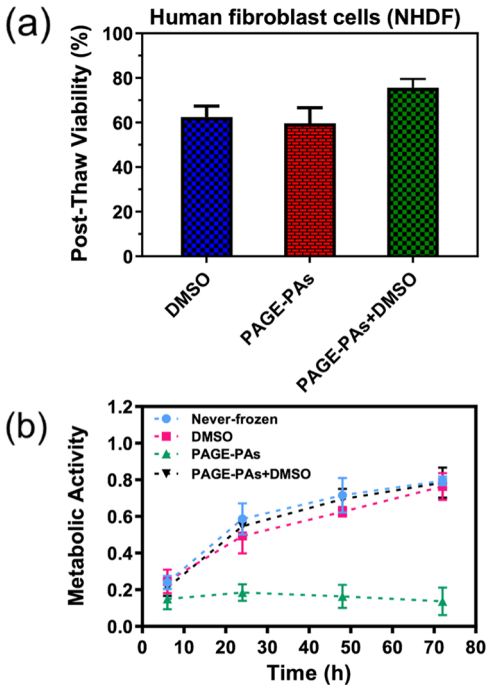

Figure 4. (a) Post-thaw survival of NHDF cells was observed to be higher in a 7% w/v PAGE-PA (35:65:0) + 3% w/v DMSO than in either 10% w/v DMSO or 10% w/v PAGE-PA. (b) Metabolic activity of 7% w/v PAGE-PA + 3% w/v DMSO was significantly higher than PAGE-PA only and marginally higher than DMSO for the first 72 h post-thaw and continued to trend higher at the end of the observation period.

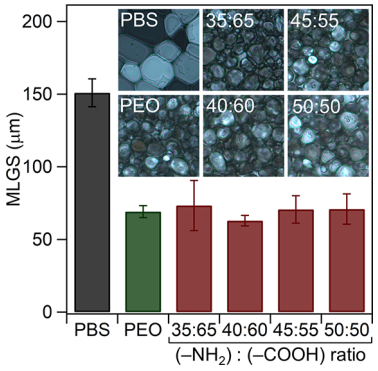

Figure 5. At 10 wt %, none of the PAGE-PAs displayed any IRI activity beyond that of PEO. The mean largest grain size (MLGS) represents the average longest linear dimension of the largest crystal within the field of view for each trial after 30 min of annealing at −6 °C. Three trials were performed for each material. Image insets are 200 μm.

was reduced, effectively putting a limit on the osmotic stress a cell would experience. Notably, at least some of the solution in the space between the ice crystals was vitrified, as evidenced in Figure 6c. The formation of a vitreous layer is expected to limit the diffusion of water and halt ice growth. Additionally, the melting onset temperature in a PAGE-PA solution (−48 °C for a 10 wt % PAGE-PA solution) is relatively high, leaving a relatively narrow temperature window in which melting occurs. In contrast, a DMSO/water solution undergoes a glass transition at ca. −130 °C, and undergoes eutectic melting at −63 °C.[56] A rapid melting process is expected to be beneficial because potentially damaging ice recrystallization occurs

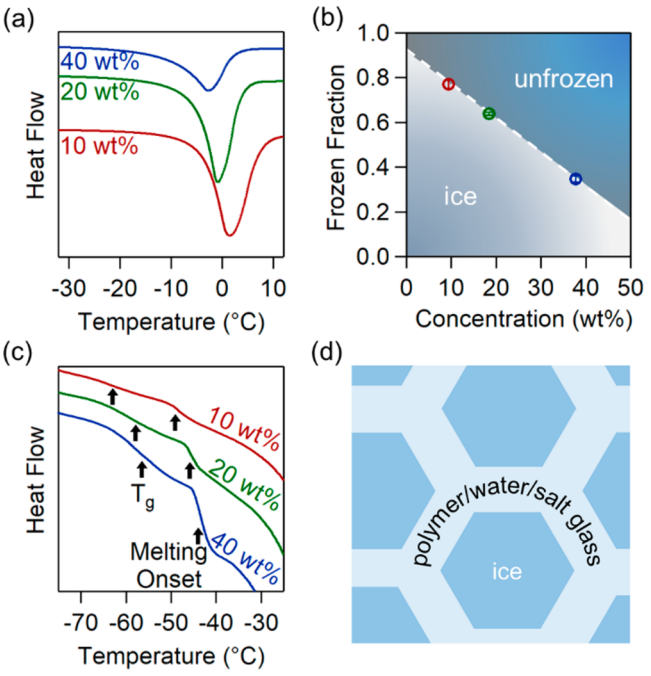

Figure 6. DSC heating traces (mass normalized; exotherms are up) for PAGE-PA (35:65 amine/carboxylic acid ratio) solutions at different concentrations. (a) Melting peaks: The area of each peak corresponds to the amount of frozen water. (b) Melting peak integrals from (a). Mass fraction of ice in each sample is calculated as wt. frac. ice = peak area/ΔH_{fusion}. (c) The unfrozen fraction (1 − wt. frac. ice) of each sample undergoes a glass transition at the indicated temperature during reheating, followed by the onset of melting. (d) Cartoon representation of a partially frozen polymer/water/buffer system.

predominantly during melting,[5] and the liquid layer between melting ice crystals has a dangerously high salt concentration.

CONCLUSION

Cryoprotective polyampholytes with a PEO backbone were shown to improve immediate post-thaw cell survival for NHDF and 3T3 cells, but long-term cell survival was poor. PEO-based polyampholytes were readily derived from poly(allyl glycidyl ether) using thiol−ene chemistry, and this synthesis platform can be readily tuned to alter pendant functionality and optimize cryoprotective properties. Immediate post-thaw viability was comparable for cells preserved with PEO-based polyampholytes and those preserved with DMSO, the most routinely used cryoprotectant for mammalian cells. Furthermore, the PEO-based polyampholytes were far less cytotoxic than DMSO, enabling their use at high concentrations to further increase post-thaw cell viability. Combining a small amount of DMSO with the most effective PAGE-PA showed promising synergy and allowed cells to proliferate competitively with never-frozen cells. Differential scanning calorimetry measurements confirm that the space between ice crystals vitrifies during freezing, limiting the total amount of frozen water and increasing the temperature at which the cell medium fully solidifies. PAGE-PA is a materials platform that can be readily tuned, modified, and used with small molecules to enable improved cryoprotection.

https://doi.org/10.1021/acs.biomac.2c01488
Biomacromolecules 2023, 24, 1475−1482

■ ASSOCIATED CONTENT

Supporting Information

The Supporting Information is available free of charge at https://pubs.acs.org/doi/10.1021/acs.biomac.2c01488.

NMR spectroscopy, SEC, characterization of regiochemistry of thiol−ene functionalization, raw post-thaw cell viability, DSC, and turbidity measurements as a function of pH (PDF)

■ AUTHOR INFORMATION

Corresponding Author

Nathaniel A. Lynd − *McKetta Department of Chemical Engineering and Center for Dynamics and Control of Materials, The University of Texas at Austin, Austin, Texas 78712, United States;* orcid.org/0000-0003-3010-5068; Email: lynd@che.utexas.edu

Authors

Aaron A. Burkey − *McKetta Department of Chemical Engineering, The University of Texas at Austin, Austin, Texas 78712, United States;* orcid.org/0000-0002-2961-8416

Neda Ghousifam − *Department of Biomedical Engineering, The University of Texas at Austin, Austin, Texas 78712, United States; Walker Department of Mechanical Engineering, The University of Texas at Austin, Austin, Texas 78712, United States*

Alexander V. Hillsley − *McKetta Department of Chemical Engineering, The University of Texas at Austin, Austin, Texas 78712, United States*

Zachary W. Brotherton − *McKetta Department of Chemical Engineering, The University of Texas at Austin, Austin, Texas 78712, United States*

Mahboobeh Rezaeeyazdi − *Department of Biomedical Engineering, The University of Texas at Austin, Austin, Texas 78712, United States; Walker Department of Mechanical Engineering, The University of Texas at Austin, Austin, Texas 78712, United States*

Taylor A. Hatridge − *McKetta Department of Chemical Engineering, The University of Texas at Austin, Austin, Texas 78712, United States*

Dale T. Harris − *McKetta Department of Chemical Engineering, The University of Texas at Austin, Austin, Texas 78712, United States*

William W. Sprague − *McKetta Department of Chemical Engineering, The University of Texas at Austin, Austin, Texas 78712, United States*

Brittany E. Sandoval − *Department of Biomedical Engineering, The University of Texas at Austin, Austin, Texas 78712, United States; Walker Department of Mechanical Engineering, The University of Texas at Austin, Austin, Texas 78712, United States*

Adrianne M. Rosales − *McKetta Department of Chemical Engineering and Center for Dynamics and Control of Materials, The University of Texas at Austin, Austin, Texas 78712, United States;* orcid.org/0000-0003-0207-7661

Marissa Nichole Rylander − *Department of Biomedical Engineering, The University of Texas at Austin, Austin, Texas 78712, United States; Walker Department of Mechanical Engineering, The University of Texas at Austin, Austin, Texas 78712, United States*

Complete contact information is available at: https://pubs.acs.org/10.1021/acs.biomac.2c01488

Notes

The authors declare no competing financial interest.

■ ACKNOWLEDGMENTS

This is a Plan II SAWIAGOS Project. This research was partially supported by the National Science Foundation through the Center for Dynamics and Control of Materials: an NSF MRSEC under Cooperative Agreement No. DMR-1720595. N.A.L. thanks the Welch Foundation for partial support of this research (F-1904). D.T.H. acknowledges support from the Green Energy At Texas (GREAT) Program provided under NSF Award CHE-1654404 to Prof. Sean T. Roberts. A.M.R. gratefully acknowledges a Career Award at the Scientific Interface (#1015895) from the Burroughs Wellcome Fund.

■ REFERENCES

(1) Israni, A. K.; Zaun, D.; Rosendale, J. D.; Schaffhausen, C.; Snyder, J. J.; Kasiske, B. L. OPTN/SRTR 2016 Annual Data Report: Deceased Organ Donation. *Am. J. Transplant.* **2018**, *18*, 434−463.

(2) Lovelock, J. E. Het Mechanism of the Protective Action of Glycerol against Haemolysis by Freezing and Thawing. *Biochim. Biophys. Acta* **1953**, *11*, 28−36.

(3) McLellan, M. R.; Day, J. G. In *Cryopreservation and Freeze-Drying Protocols*, 3rd ed.; Wolkers, W. F., Oldenhof, H., Eds.; Methods in Molecular Biology; Springer New York: New York, NY, 2015; Vol. 1257. DOI: 10.1007/978-1-4939-2193-5.

(4) Mazur, P. Kinetics of Water Loss From Cells At Subzero Temperatures and the Likelihood of Intracellular Freezing. *J. Gen. Physiol.* **1963**, *47*, 347−369.

(5) Knight, C. A.; Wen, D.; Laursen, R. A. Nonequilibrium Antifreeze Peptides and the Recrystallization of Ice. *Cryobiology* **1995**, *32* (1), 23−34.

(6) Deller, R. C.; Vatish, M.; Mitchell, D. A.; Gibson, M. I. Glycerol-Free Cryopreservation of Red Blood Cells Enabled by Ice-Recrystallization-Inhibiting Polymers. *ACS Biomater. Sci. Eng.* **2015**, *1* (9), 789−794.

(7) Wamsley, A.; Jasti, B.; Phiasivongsa, P.; Li, X. Synthesis of Random Terpolymers and Determination of Reactivity Ratios of N-Carboxyanhydrides of Leucine, ??-Benzyl Aspartate, and Valine. *J. Polym. Sci. Part Polym. Chem.* **2004**, *42* (2), 317−325.

(8) Burkey, A. A.; Riley, C. L.; Wang, L. K.; Hatridge, T. A.; Lynd, N. A. Understanding Poly(Vinyl Alcohol)-Mediated Ice Recrystallization Inhibition through Ice Adsorption Measurement and PH Effects. *Biomacromolecules* **2018**, *19* (1), 248−255.

(9) Congdon, T.; Notman, R.; Gibson, M. I. Antifreeze (Glyco)-Protein Mimetic Behavior of Poly(Vinyl Alcohol): Detailed Structure Ice Recrystallization Inhibition Activity Study. *Biomacromolecules* **2013**, *14* (5), 1578−1586.

(10) Deller, R. C.; Congdon, T.; Sahid, M. a.; Morgan, M.; Vatish, M.; Mitchell, D. a.; Notman, R.; Gibson, M. I. Ice Recrystallisation Inhibition by Polyols: Comparison of Molecular and Macromolecular Inhibitors and Role of Hydrophobic Units. *Biomater. Sci.* **2013**, *1* (5), 478.

(11) MacDonald, M. J.; Cornejo, N. R.; Gellman, S. H. Inhibition of Ice Recrystallization by Nylon-3 Polymers. *ACS Macro Lett.* **2017**, *6*, 695−699.

(12) Wowk, B.; Leitl, E.; Rasch, C. M.; Mesbah-Karimi, N.; Harris, S. B.; Fahy, G. M. Vitrification Enhancement by Synthetic Ice Blocking Agents. *Cryobiology* **2000**, *40* (3), 228−236.

(13) Wowk, B. Anomalous High Activity of a Subfraction of Polyvinyl Alcohol Ice Blocker. *Cryobiology* **2005**, *50* (3), 325−331.

(14) Graham, B.; Bailey, T. L.; Healey, J. R. J.; Marcellini, M.; Deville, S.; Gibson, M. I. Polyproline as a Minimal Antifreeze Protein Mimic That Enhances the Cryopreservation of Cell Monolayers. *Angew. Chem., Int. Ed.* **2017**, *56* (50), 15941−15944.

(15) Budke, C.; Koop, T. Ice Recrystallization Inhibition and Molecular Recognition of Ice Faces by Poly(Vinyl Alcohol). *ChemPhysChem* **2006**, *7* (12), 2601−2606.
(16) Budke, C.; Dreyer, A.; Jaeger, J.; Gimpel, K.; Berkemeier, T.; Bonin, A. S.; Nagel, L.; Plattner, C.; Devries, A. L.; Sewald, N.; Koop, T. Quantitative Efficacy Classification of Ice Recrystallization Inhibition Agents. *Cryst. Growth Des.* **2014**, *14* (9), 4285−4294.
(17) Burkey, A. A.; Hillsley, A.; Harris, D. T.; Baltzegar, J. R.; Zhang, D. Y.; Sprague, W. W.; Rosales, A. M.; Lynd, N. A. Mechanism of Polymer-Mediated Cryopreservation Using Poly(Methyl Glycidyl Sulfoxide). *Biomacromolecules* **2020**, *21* (8), 3047−3055.
(18) Smillie, J.; Munro, A.; Wood, G.; Mitchell, R. Cryopreservation of Human Platelets with Polyvinylpyrrolidone. *Transfusion (Paris)* **1981**, *21* (5), 552−556.
(19) Ting, A. Y.; Yeoman, R. R.; Lawson, M. S.; Zelinski, M. B. Synthetic Polymers Improve Vitrification Outcomes of Macaque Ovarian Tissue as Assessed by Histological Integrity and the in Vitro Development of Secondary Follicles. *Cryobiology* **2012**, *65* (1), 1−11.
(20) Takahashi, T.; Hirsh, A.; Erbe, E.; Williams, R. J. Mechanism of Cryoprotection by Extracellular Polymeric Solutes. *Biophys. J.* **1988**, *54* (3), 509−518.
(21) Stolzing, A.; Naaldijk, Y.; Fedorova, V.; Sethe, S. Hydroxyethylstarch in Cryopreservation - Mechanisms, Benefits and Problems. *Transfus. Apher. Sci.* **2012**, *46* (2), 137−147.
(22) González Hernández, Y.; Fischer, R. W. Serum-Free Culturing of Mammalian Cells–Adaptation to and Cryopreservation in Fully Defined Media. *ALTEX Altern. Zu Tierexp.* **2007**, *24* (2), 110−116.
(23) Kuleshova, L. L.; Shaw, J. M.; Trounson, A. O. Studies on Replacing Most of the Penetrating Cryoprotectant by Polymers for Embryo Cryopreservation. *Cryobiology* **2001**, *43* (1), 21−31.
(24) El-Shewy, H. M.; William, F. K.; Darrabie, M.; Collins, B. H.; Opara, E. C. Polyvinyl Pyrrolidone: A Novel Cryoprotectant in Islet Cell Cryopreservation. *Cell Transplant.* **2004**, *13* (3), 237−243.
(25) Marton, H. L.; Styles, K. M.; Kilbride, P.; Sagona, A. P.; Gibson, M. I. Polymer-Mediated Cryopreservation of Bacteriophages. *Biomacromolecules* **2021**, *22* (12), 5281−5289.
(26) Mitchell, D. E.; Lovett, J. R.; Armes, S. P.; Gibson, M. I. Combining Biomimetic Block Copolymer Worms with an Ice-Inhibiting Polymer for the Solvent-Free Cryopreservation of Red Blood Cells. *Angew. Chem. - Int. Ed.* **2016**, *55* (8), 2801−2804.
(27) Doebbler, G. F.; Buchheit, R. G.; Rinfret, A. P. Recovery and in Vivo Survival of Rabbit Erythrocytes. *Nature* **1961**, *191* (4796), 1405−1405.
(28) Hasan, M.; Fayter, A. E. R.; Gibson, M. I. Ice Recrystallization Inhibiting Polymers Enable Glycerol-Free Cryopreservation of Microorganisms. *Biomacromolecules* **2018**, *19* (8), 3371−3376.
(29) Huang, H.; Choi, J. K.; Rao, W.; Zhao, S.; Agarwal, P.; Zhao, G.; He, X. Alginate Hydrogel Microencapsulation Inhibits Devitrification and Enables Large-Volume Low-CPA Cell Vitrification. *Adv. Funct. Mater.* **2015**, *25* (44), 6839−6850.
(30) Ishibe, T.; Gonzalez-Martinez, N.; Georgiou, P. G.; Murray, K. A.; Gibson, M. I. Synthesis of Poly(2-(Methylsulfinyl)Ethyl Methacrylate) via Oxidation of Poly(2-(Methylthio)Ethyl Methacrylate): Evaluation of the Sulfoxide Side Chain on Cryopreservation. *ACS Polym. Au* **2022**, *2* (6), 449−457.
(31) Matsumura, K.; Hyon, S. H. Polyampholytes as Low Toxic Efficient Cryoprotective Agents with Antifreeze Protein Properties. *Biomaterials* **2009**, *30* (27), 4842−4849.
(32) Rajan, R.; Jain, M.; Matsumura, K. Cryoprotective Properties of Completely Synthetic Polyampholytes via Reversible Addition-Fragmentation Chain Transfer (RAFT) Polymerization and the Effects of Hydrophobicity. *J. Biomater. Sci. Polym. Ed.* **2013**, *24* (15), 1767−1780.
(33) Stubbs, C.; Lipecki, J.; Gibson, M. I. Regioregular Alternating Polyampholytes Have Enhanced Biomimetic Ice Recrystallization Activity Compared to Random Copolymers and the Role of Side Chain versus Main Chain Hydrophobicity. *Biomacromolecules* **2017**, *18* (1), 295−302.
(34) Zhao, J.; Johnson, M. A.; Fisher, R.; Burke, N. A. D.; Stöver, H. D. H. H. Synthetic Polyampholytes as Macromolecular Cryoprotective Agents. *Langmuir* **2019**, *35* (5), 1807−1817.
(35) Murray, A.; Congdon, T. R.; Tomás, R. M. F.; Kilbride, P.; Gibson, M. I. Red Blood Cell Cryopreservation with Minimal Post-Thaw Lysis Enabled by a Synergistic Combination of a Cryoprotecting Polyampholyte with DMSO/Trehalose. *Biomacromolecules* **2022**, *23* (2), 467−477.
(36) Stubbs, C.; Bailey, T. L.; Murray, K.; Gibson, M. I. Polyampholytes as Emerging Macromolecular Cryoprotectants. *Biomacromolecules* **2020**, *21* (1), 7−17.
(37) Pesenti, T.; Zhu, C.; Gonzalez-Martinez, N.; Tomás, R. M. F.; Gibson, M. I.; Nicolas, J. Degradable Polyampholytes from Radical Ring-Opening Copolymerization Enhance Cellular Cryopreservation. *ACS Macro Lett.* **2022**, *11* (7), 889−894.
(38) Rajan, R.; Hayashi, F.; Nagashima, T.; Matsumura, K. Toward a Molecular Understanding of the Mechanism of Cryopreservation by Polyampholytes: Cell Membrane Interactions and Hydrophobicity. *Biomacromolecules* **2016**, *17* (5), 1882−1893.
(39) Matsumura, K.; Hayashi, F.; Nagashima, T.; Rajan, R.; Hyon, S.-H. Molecular Mechanisms of Cell Cryopreservation with Polyampholytes Studied by Solid-State NMR. *Commun. Mater.* **2021**, *2* (1), 15.
(40) Lee, B. F.; Kade, M. J.; Chute, J. A.; Gupta, N.; Campos, L. M.; Fredrickson, G. H.; Kramer, E. J.; Lynd, N. A.; Hawker, C. J. Poly(Allyl Glycidyl Ether)-A Versatile and Functional Polyether Platform. *J. Polym. Sci. Part Polym. Chem.* **2011**, *49* (20), 4498−4504.
(41) Knight, C. A.; Hallett, J.; DeVries, A. L. Solute Effects on Ice Recrystallization: An Assessment Technique. *Cryobiology* **1988**, *25* (1), 55−60.
(42) Gibson, M. I.; Barker, C. A.; Spain, S. G.; Albertin, L.; Cameron, N. R. Inhibition of Ice Crystal Growth by Synthetic Glycopolymers: Implications for the Rational Design of Antifreeze Glycoprotein Mimics. *Biomacromolecules* **2009**, *10* (2), 328−333.
(43) Lee, J.; McGrath, A. J.; Hawker, C. J.; Kim, B.-S. PH-Tunable Thermoresponsive PEO-Based Functional Polymers with Pendant Amine Groups. *ACS Macro Lett.* **2016**, *5* (12), 1391−1396.
(44) Hunt, J. N.; Feldman, K. E.; Lynd, N. A.; Deek, J.; Campos, L. M.; Spruell, J. M.; Hernandez, B. M.; Kramer, E. J.; Hawker, C. J. Tunable, High Modulus Hydrogels Driven by Ionic Coacervation. *Adv. Mater.* **2011**, *23* (20), 2327−2331.
(45) Rahalkar, A.; Wei, G.; Nieuwendaal, R.; Prabhu, V. M.; Srivastava, S.; Levi, A. E.; de Pablo, J. J.; Tirrell, M. V. Effect of Temperature on the Structure and Dynamics of Triblock Polyelectrolyte Gels. *J. Chem. Phys.* **2018**, *149* (16), 163310.
(46) Lim, P.; Shin, H.; Moon, B.; Choi, S. H. Small Angle Neutron Scattering Study on Complex Coacervate Core Micelles Formed by Oppositely Charged Poly(Ethylene Oxide-b-Allyl Glycidyl Ether) Block Copolymer in Water. *Polym. Bull.* **2016**, *73* (9), 2417−2425.
(47) Kamoun, E. A.; Kenawy, E. R. S.; Chen, X. A Review on Polymeric Hydrogel Membranes for Wound Dressing Applications: PVA-Based Hydrogel Dressings. *J. Adv. Res.* **2017**, *8* (3), 217−233.
(48) Mitchell, D. E.; Lilliman, M.; Spain, S. G.; Gibson, M. I. Quantitative Study on the Antifreeze Protein Mimetic Ice Growth Inhibition Properties of Poly(Ampholytes) Derived from Vinyl-Based Polymers. *Biomater. Sci.* **2014**, *2* (12), 1787−1795.
(49) Mazur, P. Freezing of Living Cells: Mechanisms and Implications. *Am. J. Physiol.* **1984**, *247* (3), C125−C142.
(50) Murray, K. A.; Gibson, M. I. Post-Thaw Culture and Measurement of Total Cell Recovery Is Crucial in the Evaluation of New Macromolecular Cryoprotectants. *Biomacromolecules* **2020**, *21* (7), 2864−2873.
(51) Liu, M.; Zhang, X.; Guo, H.; Zhu, Y.; Wen, C.; Sui, X.; Yang, J.; Zhang, L. DMSO-Free Cryopreservation of Chondrocytes Based on Zwitterionic Molecule and Polymers. *Biomacromolecules* **2019**, *20*, 3980−3988.
(52) Bailey, T. L.; Stubbs, C.; Murray, K.; Tomás, R. M. F.; Otten, L.; Gibson, M. I. Synthetically Scalable Poly(Ampholyte) Which

https://doi.org/10.1021/acs.biomac.2c01488
Biomacromolecules 2023, 24, 1475−1482

Dramatically Enhances Cellular Cryopreservation. *Biomacromolecules* **2019**, *20* (8), 3104−3114.
(53) Murray, K. A.; Tomás, R. M. F.; Gibson, M. I. Low DMSO Cryopreservation of Stem Cells Enabled by Macromolecular Cryoprotectants. *ACS Appl. Bio Mater.* **2020**, *3* (9), 5627−5632.
(54) Deller, R. C.; Pessin, J. E.; Vatish, M.; Mitchell, D. A.; Gibson, M. I. Enhanced Non-Vitreous Cryopreservation of Immortalized and Primary Cells by Ice-Growth Inhibiting Polymers. *Biomater Sci.* **2016**, *4*, 1079−1084.
(55) Deller, R. C.; Vatish, M.; Mitchell, D. A.; Gibson, M. I. Synthetic Polymers Enable Non-Vitreous Cellular Cryopreservation by Reducing Ice Crystal Growth during Thawing. *Nat. Commun.* **2014**, *5*, 3244.
(56) Rasmussen, D. H.; Mackenzie, A. P. Phase Diagram for the System Water−Dimethylsulfoxide. *Nature* **1968**, *220* (5174), 1315−1317.

https://doi.org/10.1021/acs.biomac.2c01488
Biomacromolecules 2023, 24, 1475−1482